PCCP

Accepted Manuscript

ROYAL SOCIETY OF CHEMISTRY

www.rsc.org/pccp

Cite this: DOI: 10.1039/c0xx00000x

www.rsc.org/xxxxxx

ARTICLE TYPE

Double-Acceptor as a Superior Organic Dye Design for p-Type DSSCs: High Photocurrents and Observed Light Soaking Effect

Kevin A. Click‡, Damian R. Beauchamp‡, Benjamin R. Garrett, Zhongjie Huang, Christopher M. Hadad and Yiying Wu*

Received (in XXX, XXX) Xth XXXXXXXXX 20XX, Accepted Xth XXXXXXXXX 20XX
DOI: 10.1039/b000000x

Herein, we report three novel single donor double acceptor dyes, BH2, 4, and 6, for use in p-type dye sensitized solar cells (DSSCs). BH4 yields one of the highest photocurrents, 7.4 mA/cm^2, to date. The high performance is achieved *via* shorter synthetic route and no exotic materials or cell-building techniques. We suggest a structural principle when building dyes whereby one adopts a double acceptor/single anchor when a triphenylamine moiety is incorporated into a dye for p-type DSSCs. This strategy increases the molar extinction coefficient while simultaneously reducing the number of synthetic steps. The molar extinction coefficients reported herein are among the highest (99,980 M^{-1} cm^{-1}). Finally, we report the first-ever-observed light soaking effect in p-type DSSCs.

1. Introduction

Since their inception by Grätzel, M., O'Regan B. and *et. al.* DSSCs have shown much promise in the solar energy sector.[1] The most glaring advantage is their ability to surpass the so called Shockley-Queisser limit[2,3] through implementing a tandem design. The advantageous traits are not limited to the potential efficiency, but include ease of large-scale manufacture, low impurity sensitivity, and being aesthetically pleasing.

The open circuit voltage (V_{oc}) and short circuit current (J_{sc}) are two factors that contribute to the overall efficiency determination of a DSSC. In individual p- and n-type DSSCs, the maximum V_{oc} obtainable is the difference between the fermi-level of the conducting oxide and the redox potential of the electrolyte. The V_{oc} is tunable by the using different electrolytes and/or different semiconductors. Indeed, an example of the former can be seen in literature through use of a Co(II)/(III) based electrolyte to increase the V_{oc}.[4] Which has disadvantages due to the ambient air sensitivity of the cobalt species. The latter can be seen to be true through employment of p-type semiconductors such as copper gallium oxide (CGO).[5]

On the other hand maximum current obtainable from a tandem cell is limited by the lowest current producing photoactive electrode, which is currently the p-type component. Photo-cathodes (p-type DSSCs) have lower efficiencies and photo-currents owing to being less investigated. Therefore, it is desirable to increase the photo-current. This photo-current is limited by the transport resistance (charge collection efficiency) and various recombination pathways all of which can be circumvented via intelligent dye design and/or development of higher carrier mobility semiconductors compared to the commonly used NiO. Herein we focus on the intelligent dye design approach to address the photo-current limitations.

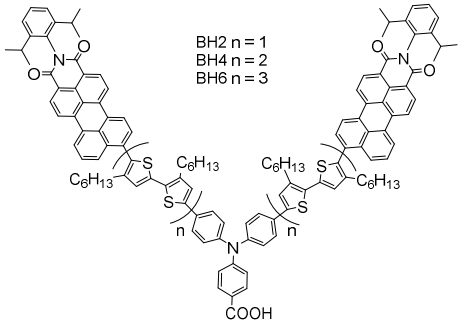

Figure 1. Structure of BH dyes.

When designing a dye for p-type DSSCs, high molar extinction coefficients are of particular importance because they reduce parasitic light absorption by NiO through use of thinner films of NiO. We envisaged that replacing a carboxylic acid anchor on the previous record holder, PMI-[BT]$_n$-TPA,[6] with an additional oligiothiophene perylene monoimide (PMI-[BT]$_n$) arm, would increase cell performance due to an increase in molar absorptivity. Device improvement due to such a concept can be seen when comparing P1 dye[7] to its analog O6[8]. P1 was a top performing dye in p-type DSSCs, O6 was synthesized two years later. The difference between these two dyes is a single acceptor and double anchor, in the case of O6, compared to the double acceptor and single anchor architecture of P1. As a result P1 has a larger molar extinction coefficient yielding better overall device performance. Therefore, a "double acceptor" dye design is suggested as the ideal design for dyes containing the triphenylamine (TPA) donor moiety. Supporting this suggestion

is the fact that synthesis of the "double acceptor" design is shorter than the single acceptor design. Thus, higher molar extinction coefficients can be achieved via less synthetic steps.

Increased device performance upon light soaking has been observed previously in the literature for both n-type and solid state DSSCs, but, to our knowledge, no such phenomena has been observed in p-type DSSCs. Similar to reports in literature, our preliminary data suggests the origin of performance increase upon light soaking in our p-type systems could be attributed to lithium cations in the redox mediator.[9–12] Our results show that when lithium is replaced by larger cations (i.e. tetrabutylammonium (TBA) and 3-hexyl-1,2-dimethylimidazolium (DMHI)) no light soaking effect is observed, such an observation has been made in solid state DSSCs.[12] The mechanism for performance increase is currently under detailed investigation.

We report photocurrent among the highest for p-type DSSCs, 7.4 mA/cm^2, with new dyes (Figure 1) whose synthetic scheme is shorter than PMI-T6-TPA.[13,14] Relative to previous record cells the NiO films used herein were prepared in the traditional manner and electrolytes used were air stable.[15] It is important to note that the dye soaking solutions used were dilute (0.01mM) and film thicknesses were between 2.0 - 2.5 μm, which is ideal when considering large scale production. Beyond that we report the first ever observed light soaking effect in p-type DSSCs, whereby performance is observed to increase to a maximum upon light soaking. The cells containing these new metastable dyes show improvement for 47 hours after which their performance is shown to be stable for weeks.

2. Results and Discussion

Synthesis and Characterization

The high molar extinction coefficients were obtainable via a shorter synthetic scheme because of the "double acceptor" design that was adopted. Where the PMI-T6-TPA has one acceptor moiety with two carboxylic anchors, the BH dyes contain two acceptor units and one carboxylic anchor. The synthetic scheme for the BH dye series can be seen in Scheme 1.

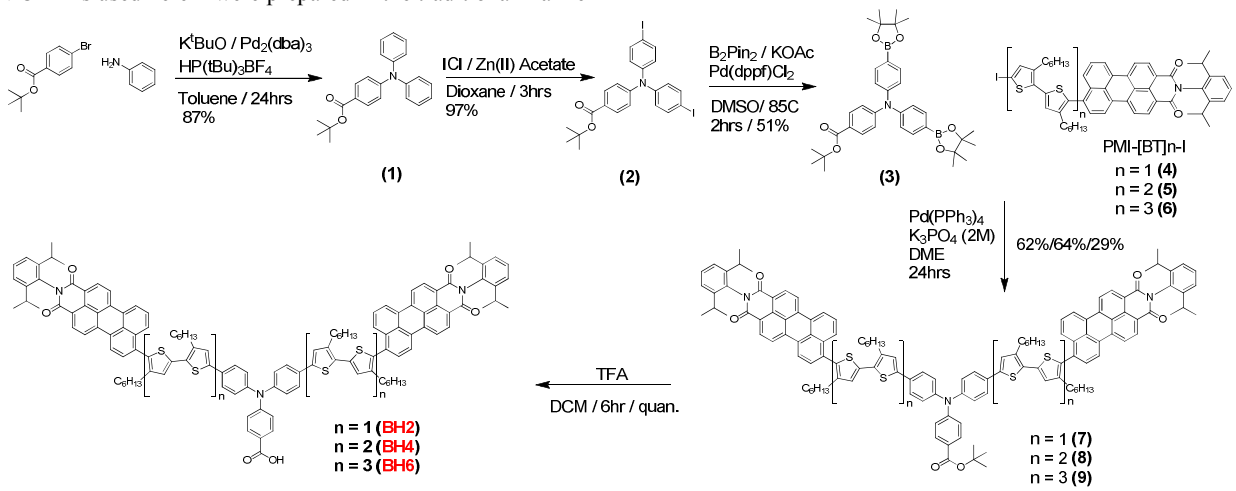

Scheme 1. Overall synthesis of the BH dye series.

The triphenylamine (TPA) moiety was synthesized starting with tert-butyl 4-bromobenzoate *via* a Buchwald-Hartwig amination with diphenylamine in high yield. The TPA unit was then iodinated with iodine monochloride in the presence of zinc acetate in almost quantitative yield. A Miyaura borylation reaction was used to synthesize the boronate pinacol ester TPA used in the subsequent reactions. This TPA unit was then used in a series of Suzuki-Miyaura couplings with PMI-[BT]$_n$-I, whose oligiothiophene length varied, to produce the ester protected dye (7, 8, & 9). All the coupling reactions employed to yield 7, 8, & 9 used the same catalyst and solvent but the temperatures were varied to minimize de-iodination products. A simple de-protection in methylene chloride with trifluoroacetic acid afforded the final BH dyes. The synthetic routes to obtain BH2, 4, & 6 are shorter by 6, 4, & 2 synthetic steps respectively when compared to PMI-T6-TPA. This fact is important with respect to the large scale production, as the synthetic route for obtaining the dyes for these devices needs to be as short as possible to help keep production costs low. The UV-vis data in methylene chloride can be seen Figure 2. BH2, 4, & 6 have maximum

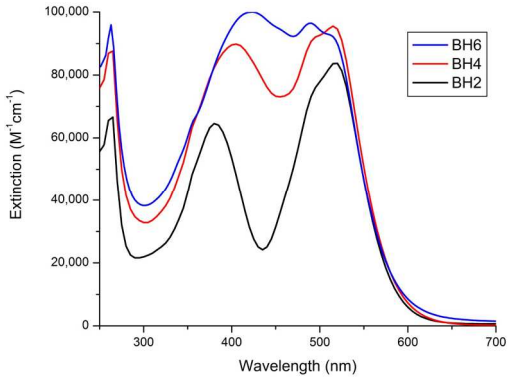

Figure 2. UV-vis of BH series dyes in methylene chloride.

absorption at 520, 515, and 488 nm, corresponding to molar

extinction coefficients of 8.4 x 10^4, 9.6 x 10^4, & 9.6 x 10^4 $M^{-1}cm^{-1}$, respectively. The absorption peaks at 265, 486 and 509 nm correspond mainly to the π-π* N-(2,6-diisopropylphenyl)perylene-3,4-dicarboximide (PMI) with the charge transfer absorption at the longer wavelength shoulder at 520 nm with an absorption peak rising at 375 nm corresponding to the π-π* of the oligiothiophene bridge.[16] These peaks increase in intensity from BH2-BH6 as the length of the conjugated oligiothiophene double acceptor is lengthened.

A bathochromic shift is noticed as the oligiothiophene bridge is extended. This can be attributed to a more negative shift of the highest occupied molecular orbital (HOMO) energy level due to increased conjugation with the lowest unoccupied molecular orbitals (LUMO) energy remaining constant. This is supported by both the cyclic voltammogram (S1 in S.I.) and the DFT calculations which illustrate HOMO location on the TPA-oligiothiophene donor.

The BH series dyes show similar shape in UV-vis absorption spectra compared to the single acceptor/double anchor design of the PMI-$[BT]_n$-TPA dye, but the BH dyes show both increased molar extinction coefficients as well as bathochromic shifts. Again, this is attributed to an increase in conjugation due to two π-linker bridges, opposed to two anchoring groups (COOH) of the PMI-$[BT]_n$-TPA single acceptor model.

Emission spectra (S3 in S.I.) were obtained in 0.01 mM methylene chloride solutions at room temperature with excitation wavelengths corresponding to absorption wavelength maximums as described in Table 1. The stokes shift for BH2, BH4 and BH6 were 81, 66, and 87 nm respectively. The intersection of the normalized fluorescence spectra and absorption spectra were taken to be the $E_{0\text{-}0}$ of the dyes which can be seen in Table 1.

Dye	BH2	BH4	BH6
$\lambda_{abs,\,max}$ (nm)/ ε ($M^{-1}cm^{-1}$)	380/64,580; 520/83,700	405/89,830; 515/95,510	422/99,980; 488/96,450
$\lambda_{em,\,max}$ (nm)	604	581	575
E^0_{ox} (V vs NHE)	1.18	1.16	1.14
E^0_{red} (V vs NHE)	-0.65	- 0.64	- 0.65
$E_{0\text{-}0}$[a] (eV)	2.25	2.28	2.27
$E(S^*/S^-)$[b] (V vs NHE)	1.60	1.64	1.62
$\Delta E_{opt.}$[c]	2.12	2.11	2.11

Table 1. Summary of optical and electrochemical properties of the dyes. [V] vs NHE. (a) $E_{0\text{-}0}$ taken to be intersection of absorption and normalized emission spectra. (b) $(S^*/S^-) = E_{0\text{-}0} + E^o_{red}$. (c) Determined from the start of absorption of the longer-wavelength shoulder absorption.

DFT Calculations

Structure and conformation, along with electron density distribution, of the BH series dyes were studied using density functional theory (DFT) with B3lyp level of theory with 6-31G basis sets. As shown in Figure 3, the electron density distribution of the LUMO for the three dyes were quite similar to each other and were significantly localized on the PMI unit. The dihedral angles between thiophene units in the oligiothiophene arms of the BH dyes are not symmetric. This likely accounts for the observation that the LUMO resides on only one arm of the BH dyes. The LUMO+1 orbital in all cases exhibit electron density located on the opposite arm, where the energies between LUMO and LUMO+1 are small. Additionally, the HOMO for the three dyes were quite similar, where the electron density is delocalized across the oligiothiophene arms.

Solution Electrochemistry

The electrochemistry of all the dyes was obtained using cyclic voltammetry in methylene chloride. The dyes show reversible first oxidation peaks corresponding to the oxidation of the donor triphenylamine and oligiothiophene moiety where DFT calculations show HOMO orbital location (see figure 3 for DFT). The first oxidation peak shifts are 1.18, 1.16, and 1.14 V vs. NHE, for BH2, BH4, and BH6 respectively. This first oxidation shifts more negative going from BH2 to BH6. This could be explained by increased radical cation delocalization across the conjugated oligiothiophene units, lowering the energy needed to oxidize the donor moiety.

Also, HOMO location of BH2 is more localized near the electron withdrawing anchor (COOH), affording a more positive oxidation potential. As the oligiothiophene chain is increased, the HOMO moves away from the TPA unit where the carboxylic acid anchor resides and spreads across the oligothiophene chain hence increasing conjugation of the HOMO and increasing the distance from the carboxylic acid. The PMI-$[BT]_n$-TPA show the same trend in that the HOMO negatively shifts with increasing conjugation of the oligiothiophene bridges as expected, but the BH series dyes show a more positive HOMO shift, possibly due to proximity of the carboxylic acid anchoring group and less delocalization of the HOMO.

A more complex irreversible oxidation of the donor moiety can be seen at more positive potentials where radical dications and trications exist, but herein the focus was on the frontier oxidations and reductions. Reversible reduction peaks corresponding to reduction of the PMI acceptor unit can be observed at -0.66, -0.64, and -0.65 V with reference to NHE for BH2, BH4 and BH6, respectively. The reduction potentials remain relatively constant as the oligiothiophene chain is extended, meaning the PMI acceptor moiety is independent of the donor subunit's electronic character. This is consistent with DFT calculations which show the LUMO is localized on the PMI moiety. The same trend was observed for the PMI-$[BT]_n$-TPA. Electrochemical measurements are summarized in Table S2 in the supporting information. Electrochemical and optical measurements show that the energy alignments of BH2, 4 and 6 all have a large driving force for hole injection into NiO (~0.5 V vs. NHE) and a favourable regeneration energy for the redox mediator I^-/I_3^- (~0.35V vs NHE).

Solar Cell Fabrication and Performance

The solar cells yielding high photocurrents were fabricated using common morphology NiO (2.0 - 2.5 μm thick film) opposed to the, synthetically more cumbersome, NiO microballs (6.0 μm thick film) employed to achieve a previous high photocurrent using PMI-T6-TPA.[15] The NiO films were soaked overnight in 0.01 mM dye solutions. The electrolyte used was a 1.0 M 3-hexyl-1,2-dimethylimidazolium iodide (DMHII) with 0.1 M iodine in acetonitrile. A more detailed description of solar cell

Cite this: DOI: 10.1039/c0xx00000x

www.rsc.org/xxxxxx

ARTICLE TYPE

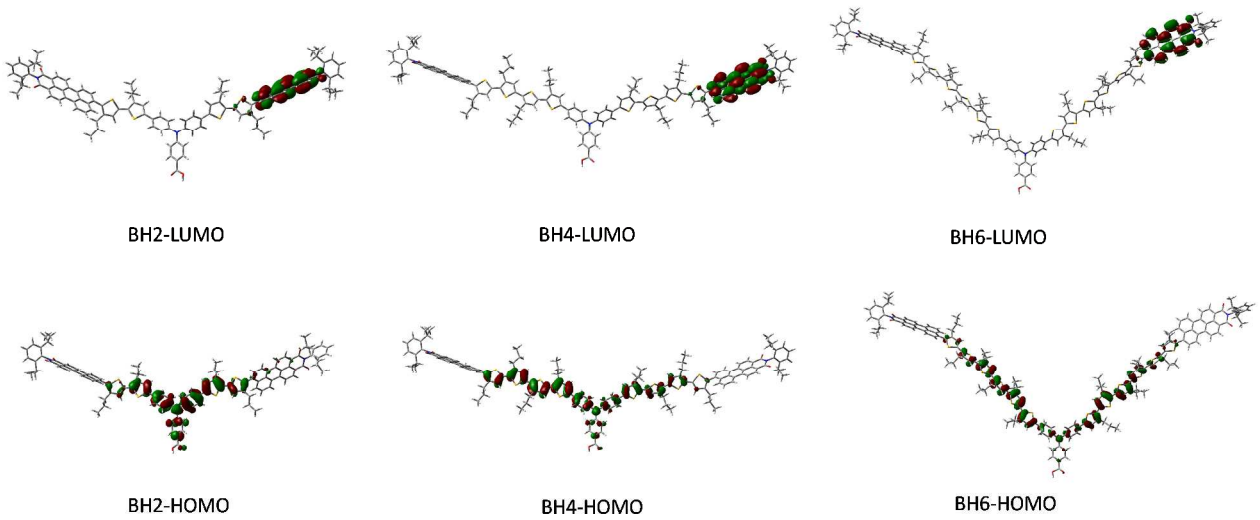

Figure 3. DFT calculations with B3lyp level of theory with 6-31G basis sets

fabrication can be found in the experimental section.

To begin a comparison between the double acceptor and single acceptor design was investigated using the shortest bithiophene linker between the donor and acceptor. The results can be seen in table 2. As a result of the BH2's superior performance this double acceptor design was further investigated.

Dye	ε (M^{-1} cm^{-1})^X	J_{sc} (mA/cm^2)^Y	V_{oc} (mV)^Y	η^Y
PMI-BT-TPA	35,440	2.7	97	0.08
BH2	57,120	4.5	126	0.21

Table 2. Comparison between single acceptor (PMI-BT-TPA) and double acceptor variant (BH2). (**X.** UV-vis data in DMF; **Y.** Electrolyte (I^-/I_3^-)

Figure 4 shows the J-V curves of the solar cells containing BH series dyes. BH4 shows the best performance with a J_{sc} of 7.4 mA/cm^2, V_{oc} of 128 mV, and a fill factor (FF) of 0.30 resulting in an overall efficiency (η) of 0.28. BH2 and BH6 had very similar performance among themselves with a J_{sc} of 4.3 and 4.4 mA/cm^2 and a V_{oc} of 97 and 95 mV, respectively, resulting in a fill factor of 0.31 and an efficiency of 0.13 for both BH2 and BH6. Table 3 summarizes the solar cell results.

The increased device performance is attributed to the increased molar extinction coefficients of the BH dyes (8.4 x 10^4 to 9.6 x 10^4 $M^{-1}cm^{-1}$) compared to the single acceptor dye design used in PMI-T6-TPA (6.7 x 10^4 $M^{-1}cm^{-1}$). It was initially thought upon designing the BH dye series, that device performance might suffer due to low dye loading because of increased steric bulk.

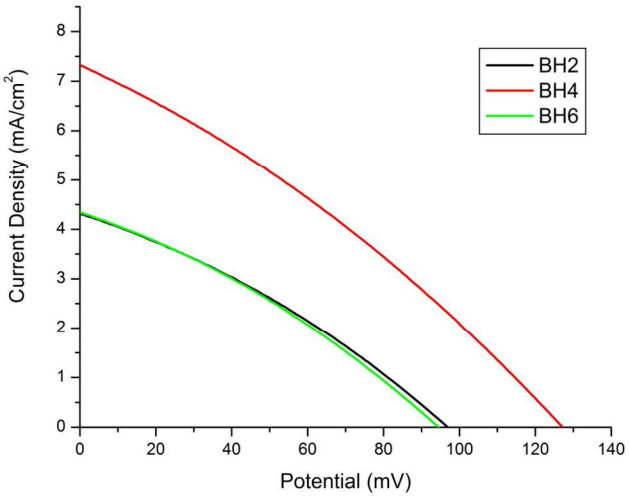

Figure 4. J-V curve of dyes with cells constructed with 1.0M DMHII / 0.1M iodine electrolyte in acetonitrile.

Dye	J_{sc} (mA/cm^2)	V_{oc} (mV)	FF	η
BH2	4.3	97	0.31	0.13
BH4	7.4	128	0.30	0.28
BH6	4.4	95	0.31	0.13

Table 3. Summary of cell results using DMHII electrolyte.

We found that BH2, 4 and 6 loaded 25 ± 1, 22 ± 3, 8.4 ± 6 $nmol/cm^2$ respectively. The adsorption measurements were obtained via UV-vis measurements before and after film soaking. The observation that one anchoring group is sufficient for good

Dye	BH2	BH4	BH6
$\lambda_{abs,\,max}$ (nm)/ ε ($M^{-1}cm^{-1}$)	380/64,580; 520/83,700	405/89,830; 515 95,510	422/99,980; 488/96,450
Dye loading (nmol cm^{-1})	25 ± 1	22 ± 3	8.4 ± 6
Jsc	4.3	7.4	4.4

Table 4. Relation between dye loading and molar extinction on photocurrent.

dye loading is further supported by the very dilute soaking solution used in this study. These results indicate one anchoring group is sufficient for good dye loading and performance.

Molar extinction coefficients cannot entirely explain the performance of the dyes due to the fact that BH4 has a significantly increased J_{sc} when compared to BH2 and BH6 which have similar J_{sc} but much different molar extinction coefficients. Extending to six thiophenes (BH6) maximizes light absorption, but caused decreased dye loading (BH2, 4 and 6 loaded 25 ± 1, 22 ± 3, 8.4 ± 6 nmol/cm^2). There was found to be a balance between dye loading and the molar extinction coefficient. Evidence of this balance can be seen in table 4 where BH2 and BH6 have similar J_{sc} values but BH6's larger molar extinction coefficient, compared to BH2, is negated by the fact that dye loading is lower due to the significantly increased steric bulk.

Lastly the increased oligiothiophene length of BH6 has enough degrees of freedom that one could envisage the acceptor moiety coming in contact with the NiO surface. It is also possible that only two thiophenes (BH2) inadequately shields the surface of NiO. Increasing the length of the oligiothiophene bridge can create more hydrophobic bulk due to the hexyl chains, which has been shown to decrease recombination between the redox mediator and semiconductor surface.[17–22] Moreover, extending the oligiothiophene length can prevent recombination by increasing the electron tunnelling distance between the electron located in the excited state LUMO of the dye and vacancies on the NiO surface.[8,21] Performance of the cell was maximized when the oligiothiophene bridge contained four thiophenes (BH4) which indicates a balance between all of these factors was obtained.

Cation Effect/Light Soaking

Next, solar cells using the best performing dye (BH4) were fabricated using 3 different 1.0 M electrolytes each having the same iodide anion but varying cations being **lithium, TBA**, and **DMHI**. Each electrolyte had the same concentration of iodine (0.1M). The film thickness for the cells were between 2.0 and 2.2 µm thick. Figure 5 shows the J-V curve for the three cells and Table 5 summarizes the results. The DMHII electrolyte cell gave similar results when compared to the prior solar cell data described above in that the J_{sc} was 7.2 mA/cm^2, V_{oc} was 116 mV, and the fill factor was 0.30 with a resulting efficiency of 0.25. The two other electrolytes containing LiI and TBA showed almost identical performance with a J_{sc} of 6.41 and 6.46 mA/cm^2 and a V_{oc} of 124 and 126 mV resulting in a fill factor of 0.32 and 0.29 respectively, and efficiencies of 0.25 for both cells.

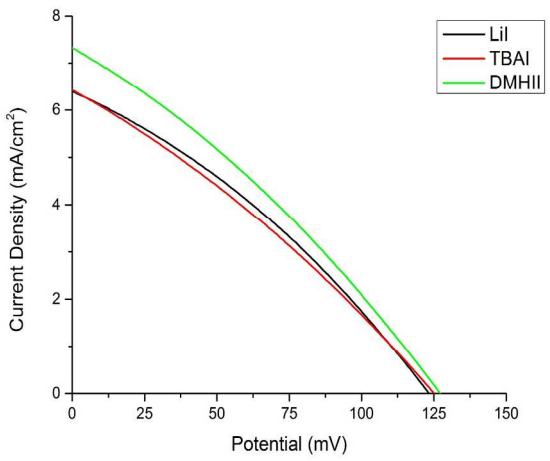

Figure 5. J-V curve of BH4 with 1.0M LiI, TBAI, and DMHII and 0.1M iodine in acetonitrile.

Cation	J_{sc} (mA/cm^2)	V_{oc} (mV)	FF	η
TBA	6.5	126	0.29	0.24
Li	6.4	124	0.32	0.25
DMHI	7.4	128	0.31	0.28

Table. 5. Performance results of BH4 in the J-V curve shown in Fig. 5.

The most interesting result of the different electrolytes used was the observed light soaking effect for the cell in the presence lithium cations. The lithium cation containing cell shows an increase in current as a function of time until a plateau is reached and no increase in current is observed. Table 6 summarizes the results of the 3 cells. Nine cells were constructed with three dyes (3 cells per dye) and a detailed time/light soaking study was conducted, whereby the cells were tested approximately every 8 hours. At the beginning of each test, chronoamperometry was conducted until the current increase due to light soaking reached a consistent maximum. Then, JV data was collected followed by impedance data. Once the initial testing for the cells was complete, they were stored in the dark until the next testing. It was found that over 47 hours of testing the transport resistance continually decreased while the short circuit current increased (Figure 6). The V_{oc} of BH2 and BH4 remained relatively constant but the V_{oc} for BH6, the largest dye, increased over the light soaking treatments (S.I. Figure S4). In addition, we observed a significant difference in the capacitance of the cells. The cell that contained lithium cations had a much larger capacitance (S.I. Figure S5). The mechanism for performance increase is currently under detailed investigation.

Cation	J_{sc} (mA) initial	J_{sc} (mA) at 47 hours	Δ (mA)
TBA	1.796	1.802	0.006
Li	1.771	1.794	0.023
DMHI	2.009	2.017	0.008

Table 6. Chronoamperometry results of BH4 during light soaking process.

Cite this: DOI: 10.1039/c0xx00000x

www.rsc.org/xxxxxx

ARTICLE TYPE

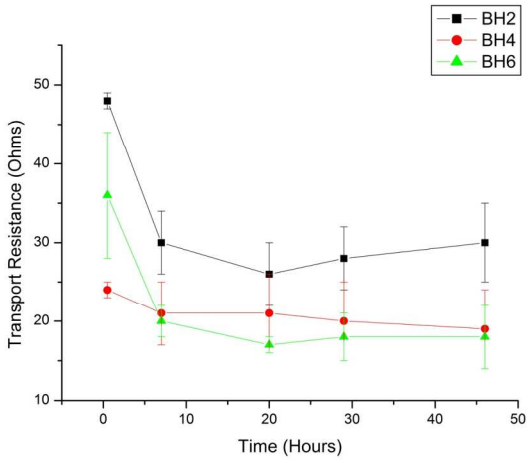

Figure 6. Transport resistance measured at V_{oc} as a function of light soaking time.

3. Experimental

General Information

All synthetic reagents, solvent, and silica were purchased from either Sigma-Aldrich or Fisher Scientific with the exception of tert-Butyl 4-bromobenzoate which was purchased from Frontier. Scientific. 3-hexyl-1,2-dimethylimidazolium iodide (DMHII) was purchased from Solaronix. All products were characterized by ^{1}HNMR and 13CNMR using a Avance III 400 instrument and ESI-MS was utilized by a BrukerMicroTOF (ESI) outfitted with an Agilent 1200 LC. MALDI-MS was obtained usinga Bruker-Daltonics UltrafleXtreme MALDI-TOF-TOF MS.

Photophysical Measurements

All solutions were 0.01 mM in methylene chloride and taken at room temperature. UV-Vis absorption of dye solutions were obtained using a Perkin Elmer Lambda 950 instrument. Emission spectra were obtained using a Fluoromax-4 from Horiba Scientific instrument with an excitation wavelength corresponding to the maximum absorbance for each dye which can be seen in Table 1.

Electrochemical Measurements

Cyclic voltammetry was obtained using a Gamry potentiostat. All dye solutions were 0.1 mM in anhydrous methylene chloride with a 0.1 M tetrabutyl ammonium hexafluorophosphate supporting electrolyte which were purged with argon 20mins prior to scans. The scan rate for all cyclic voltammograms was 100 mV/s. The working electrode, counter electrode and reference electrode were a Pt dish, Pt mesh, and a 0.01 M Ag/AgNO3 electrode respectively. The reference electrode was calibrated using ferrocene as the internal standard ($E°(Fc^+/Fc)$ = 0.640 V vs NHE).

Cell Fabrication

The NiO films were prepared using a modified sol-gel method.[25,26,27] The green sol-gel solution was then doctor bladed on to FTO glass and heated at 450°C for 30mins. Film thickness was varied by repeated cycles of doctor blading and heating. Film thickness was determined using a AlphaStep D-100 profilometer from KLA-Tencor corporation. Pt counter electrodes with predrilled holes were prepared by thermal deposition of a 25 µM H_2PtCl_6 solution in isopropyl alcohol on FTO glass at 385°C for 20 minutes. NiO films were soaked overnight in 0.01 mM dye solutions in DMF for BH2 and BH4 and methylene chloride for BH6. The sensitized films were then washed with either DMF (BH2 and BH4 films) or methylene chloride (BH6 films), and air dried. The cell was assembled by sandwiching Surlyn60 film between the working and counter electrode which was clamped and heated. Electrolyte was injected through the predrilled hole of the counter electrode under vacuo. The hole was then sealed by heating a Surlyn60 film under a thin glass slide. J-V curves were measured under 100 $mWcm^{-2}$ AM 1.5 illumination generated by a solar simulator (Small-Area Class B, Solar Simulator, PV Measurements, Inc.).

Methods for light soaking study

Nine cells were assembled using the three BH dyes (3 cells per dye). Chornoamperometry was carried out first by light soaking the cells at open circuit conditions. Next, J-V curves were measured followed by impedance measurements. This general sequence of testing was followed for all cells every 8 hours until the light soaking effect was no longer observed. After each test sequence, the cells were stored in a dry dark place until the next test.

Adsorption Study

Nine NiO films were constructed as described above with thicknesses between 1.8-1.9 µm thick for all films. A volumetric pipet was used to measure exactly 10.00mL of each dye solution (0.01mM for all dyes, BH2 and BH4 in DMF and BH6 in methylene chloride) in which 3 films for each dye was soaked in individual 10.00 mL dye solutions. Using the known molar exctinction coeffients of the dyes, concentrations of the solutions before and after soaking were determined via the UV-Vis spectrometer described above to determine amount of dye loaded onto the NiO surface.

Synthesis

Tert-butyl 4-(diphenylamino)benzoate (1). To an oven dried 250 mL 3-neck round bottom flask containg a stir bar was charged with potassium tert-butoxide (4.18 g, 37.2 mmol),

diphenylamine (3.00 g, 17.7 mmol), and tert-butyl 4-bromobenzoate (4.92 g, 19.2 mmol). The flask was fitted with septa, purged with argon (3x's), toluene (88 mL) was added at once via syringe, and the system was purged with argon once more. Next, $Pd_2(dba)_3$ (811 mg, 886 μmol) and $HP(^tBu)_3BF_4$ (514 mg, 1.77 mmol) we added together at once and the system was purged with argon (3x's). The solution was allowed to stir (24 hours), after which it was poured into water (100 mL) and the organic layer was separated. The aqueous layer was extracted with methylene chloride (3 x 75 mL), the organic extracts were combined, dried over $Mg(SO_4)_2$, filtered, and concentrated in vacuo. The crude solid was purified via column chromatography using on eluent of methylene chloride/hexanes yielding white solid (5.35 g, 87%). ^{1}HNMR (400MHz, $CDCl_3$): δ = 7.82 (d, 2H, J = 8.88 Hz), 7.32-7.26 (m, 4H), 7.15 -7.07 (m, 6H), 6.99 (d, 2H, J = 8.84 Hz), 1.57 (s, 9H). ^{13}CNMR (400MHz, $CDCl_3$): δ = 165.76, 151.76, 147.02, 130.79, 129.63, 125.72, 124.53, 124.29, 120.58, 80.51, 28.41. MS (ESI-TOF): m/z $[M + Na^+]$ = 368.16

Tert-butyl 4-(bis(4-iodophenyl)amino)benzoate (2). To a 250 mL single neck round bottom flask containing a stir bar was charged with dioxane (62 mL), Zn (II) acetate (5.31 g, 28.9 mmol), and ICl (2.65 mL, 51.0 mmol, 3.10 g/mL). The flask was fitted with dropping funnel containing **1** (5.00 g, 14.5 mmol) dissolved in dioxane (24 mL) and the solution was added dropwise (2 hours). The resulting solution was allowed to stir for 3 hours. After which the reaction solution was poured into sodium thiosulfate (1M, 400 mL), the organic layer was separated, and the aqueous was extracted with methylene chloride (3 x 100 mL). The organic extracts were combined, dried over $Mg(SO_4)_2$, filtered, and concentrated in vacuo. The resulting dark grey solid was filtered over a column of silica using methylene chloride as the eluent yielding a light grey solid (8.30 g, 96%). M.P.: 180 ºC. ^{1}HNMR (400MHz, $CDCl_3$): δ = 7.84 (d, 2H, J = 8.84 Hz), 7.57 (d, 4H, J = 8.80), 7.00 (d, 2H, J = 8.84 Hz), 6.85 (d, 4H, J = 8.80 Hz), 1.57 (s, 9H). ^{13}CNMR (400MHz, $CDCl_3$): δ = 165.43, 150.57, 146.44, 138.73, 131.01, 127.05, 126.07, 121.82, 87.67, 80.85, 28.38. MS (ESI-TOF): m/z $[M + Na^+]$ = 619.96

Tert-butyl 4-(bis(4-(4,4,5,5-tetramethyl-1,3,2-dioxaborolan-2-yl)phenyl)amino)benzoate (3). A 50 mL round bottom flask containing a stir bar was charged with **2** (1.00 g, 1.67 mmol), bis(pinacolato)diboron (1.06 g, 4.19 mmol), potassium acetate (1.23g, 13.0 mmol), and $Pd(dppf)Cl_2$ (137 mg, 167 μmol). The flask was taken into a glove box where DMSO (17 mL) was introduced, the flask was sealed, and taken out of the glove box. The flask was purged with argon and light brown solution was heated whilst stirring (85ºC, 2 hours). After which the solution was allowed to cool to room temperature and filtered over a plug of silica washing with methylene chloride. The filtrate was concentrated in vacuo and precipitated from hot methanol. The precipitate was filtered yielding white solid (510 mg, 51%). M.P.: 241 ºC decomp. ^{1}HNMR (400MHz, $CDCl_3$): δ = 7.83 (2H, J = 8.84 Hz), 7.71 (4H, J = 8.52 Hz), 7.08 (4H, J = 8.48 Hz), 7.05 (2H, J = 8.84 Hz), 1.58 (s, 9H), 1.34 (s, 24H). ^{13}CNMR (400MHz, $CDCl_3$): δ = 165.62, 151.06, 149.53, 136.22, 130.83, 125.98, 124.12,122.66, 83.90, 80.76, 28.40, 25.02. MS (ESI-TOF): m/z $[M + Na^+]$ = 620.33

2-(2,6-diisopropylphenyl)-1H-benzo[5,10]anthra[2,1,9-def]isoquinoline-1,3(2H)-dione. Was synthesized following procedures from literature.[28]

8-bromo-2-(2,6-diisopropylphenyl)-1H-benzo[5,10]anthra[2,1,9-def]isoquinoline-1,3(2H)-dione. Was synthesized following procedures from literature.[29]

Synthesis of 4, 5, and 6.
Were synthesized following procedures from literature.[16]

General procedure for synthesis of compounds 7, 8, and 9. A 10 mL round bottom containing a stir bar was charged with PMI-$[BT]_n$-I (n = 1, 2, and 3 for **4**, **5**, and **6** respectively), **3** (TPA), tripotassium phosphate, and dimethoxyethane. The vessel was sealed with a septa and purged with argon. Next, $Pd(PPh_3)_4$ was added, the solution was purged with argon, and heated (24 hours). The solutions were allowed to cool to room temperature, poured in water, the organic layer was removed, and the aqueous layer was extracted with ethyl acetate for **7** or methylene chloride for **8** and **9**. The combined organic extracts were concentrated in vacuo yielding deep red solid, which was purified via column chromatography over silica using a methylene chloride eluent. A deep black crystalline material was obtained from the column.

Tert-butyl-4-(bis(4-(5'-(2-(2,6-diisopropylphenyl)-1,3-dioxo-2,3-dihydro-1H-benzo[10,5]anthra[2,1,9-def]isoquinolin-8-yl)-3,4'-dihexyl-[2,2'-bithiophen]-5-yl)phenyl)amino)benzoate (7). Following the general procedure, PMI-$[BT]_n$-I (4) (433mg, 461μmol), TPA (3) (125mg, 209μmol), and tripotassium phosphate (2M, 1.46mmol) were dissolved in dimethoxyethane (3mL) in the presence of catalyst (48mg, 42 μmol) to yield the title compound (255mg, 62%). M.P.: 185 ºC. ^{1}HNMR (400MHz, $CDCl_3$): δ = 8.66 (d, 4H J = 8.00), 8.49-8.42 (m, 8H), 8.02 (d, 2H, J = 8.52Hz), 7.91 (d, 2H, J = 8.84Hz), 7.70 (d, 2H, J = 7.76Hz), 7.64 (t, 2H, J = 15.9Hz), 7.57 (d, 4H J = 8.64Hz), 7.50 (t, 2H, J = 7.78Hz),7.36 (d, 4H, J = 7.72Hz), 7.21-7.16 (m, 6H), 7.13 (d, 2H J = 8.80Hz), 2.91-2.76 (m, 8H), 2.47 (t, 4H, J = 7.52Hz), 1.76 (quin, 4H), 1.62 (s, 12H), 1.51-1.42 (m, 5H), 1.41-1.31 (m, 10H), 1.30-1.26 (approx. s, 6H), 1.22 (approx. d, 36H, J = 6.84 Hz), 0.91 (t, 7H, 6.94 Hz), 0.79 (t, 6H, 6.92 Hz). ^{13}CNMR (400MHz, $CDCl_3$): δ = 165.69, 164.14, 151.08, 146.17, 145.91, 142.17, 141.43, 140.85, 137.69, 137.42, 136.40, 135.12, 134.07, 132.23, 131.25, 131.04, 130.69, 130.58, 130.11, 130.03, 129.66, 129.59, 129.55, 128.45, 127.50, 127.33, 127.07, 126.81, 126.12, 125.64, 124.23, 123.3, 121.76, 121.32, 121.26, 120.59, 120.50, 80.84, 31.92, 31.70, 30.81, 30.68, 29.91, 29.50, 29.38, 29.25, 29.14,28.48, 24.24, 22.85, 22.69, 14.32, 14.21. MS (MALDI-TOF): m/z $[M^+]$ = 1967.8

Tert-butyl-4-(bis(4-(5'''-(2-(2,6-diisopropylphenyl)-1,3-dioxo-2,3-dihydro-1H-benzo[10,5]anthra[2,1,9-def]isoquinolin-8-yl)-3,4',4'',4'''-tetrahexyl-[2,2':5',2'':5'',2'''-quaterthiophen]-5-yl)phenyl)amino)benzoate (8). Following the general procedure, PMI-$[BT]_n$-I (5) (445mg, 350μmol), TPA (3) (87mg, 146μmol), and tripotassium phosphate (2M, 1.02mmol) were dissolved in dimethoxyethane (2mL) in the presence of catalyst (34mg,

29μmol) to yield the title compound (247mg, 64%). M.P.: 198 ºC. ^{1}HNMR (400MHz, $CDCl_3$): δ = 8.69 (d, 4H, J = 7.96 Hz), 8.56-8.47 (m, 8H), 8.02 (d, 2H, J = 8.48 Hz), 7.88 (d, 2H, J = 8.68 Hz), 7.72 (d, 2H, 7.72 Hz), 7.67 (t, 2H, J = 7.94 Hz), 7.57-7.51 (m, 4H), 7.49 (t, 2H, J = 7.49 Hz), 7.35 (d, 4H, J = 7.80 Hz), 7.19-7.08 (m, 9H), 7.02 (d, 5H, J = 5.56 Hz), 2.89-2.75 (m, 15H), 2.46 (t, 4H, J = 7.60 Hz), 1.79 (m, 12H), 1.62-1.57 (approx. s, 12H), 1.50-1.41(m, 12H), 1.40-1.30 (m, 26H), 1.20 (approx. d, 36H, J = 6.84 Hz), 0.95-0.87 (m, 18H), 0.78 (t, 6H J = 6.86 Hz). ^{13}CNMR (400MHz, $CDCl_3$): δ = 164.12, 145.87, 142.14, 41.28, 140.79, 140.10, 137.73, 137.46, 136.02, 135.09, 134.28, 134.18, 134.08, 132.24, 131.20, 130.95, 130.70, 130.55, 130.02, 129.60, 128.77, 128.68, 128.45, 127.94, 127.48, 127.36, 127.10, 126.73, 126.05, 125.56, 124.23, 124.16, 123.28, 121.31, 121.24, 120.60, 120.52, 31.86, 31.64, 30.73, 30.67, 30.62, 29.79, 29.67, 29.42, 29.30, 29.18, 29.07, 28.42, 24.18, 22.80, 22.64, 14.28, 14.15. MS (MALDI-TOF): m/z [M^+] = 2632.2

Tert-butyl-4-(bis(4-(5'''''-(2-(2,6-diisopropylphenyl)-1,3-dioxo-2,3-dihydro-1H-benzo[10,5]anthra[2,1,9-def]isoquinolin-8-yl)-3,4',4'',4''',4'''',4'''''-hexahexyl-[2,2':5',2'':5'',2''':5''',2'''':5'''',2'''''-sexithiophen]-5-yl)phenyl)amino)benzoate (9). Following the general procedure, PMI-$[BT]_n$-I (6) (148mg, 92μmol), TPA (3) (25mg, 42μmol), and tripotassium phosphate (2M, 293μmol) were dissolved in dimethoxyethane (1mL) in the presence of (15mg, 13μmol) to yield the title compound as a dark red solid (40mg, 29%). M.P.: 153 ºC. ^{1}HNMR (400MHz, $CDCl_3$): δ = 8.68 (d, 4H, J = 7.88 Hz), 8.54 (m, 8H), 8.03 (d, 2H, J = 8.44 Hz), 7.90 (d, 2H, J = 8.72 Hz), 7.71 (d, 2H, J = 7.72 Hz), 7.66 (t, 2H, 7.88 Hz), 7.54 (d, 4H, J = 8.48 Hz), 7.50 (t, 2H, J = 7.82 Hz), 7.37 (d, 4H, J = 7.76 Hz), 7.23-7.09 (m, 10H), 7.08-6.98 (m, 8H). 2.92-2.75 (m, 20H), 2.48 (t, 4H, J = 7.38 Hz), 1.81-1.68 (m, 16H), 1.62 (s, 12H), 1.51-1.43 (m, 16H), 1.41-1.32 (m, 38H), 1.27 (approx. s, 8H), 1.22 (approx. d, 30H), 0.97-0.88 (m, 28H), 0.80 (t, 6H, J = 6.85 Hz). ^{13}CNMR (400MHz, $CDCl_3$): δ = 164.08, 145.85, 142.12, 141.22, 140.74, 137.67, 134.02, 137.39, 136.01, 135.06, 134.16, 134.02, 133.95, 132.17, 131.19, 130.95, 130.64, 130.56, 130.04, 129.55, 128.74, 128.65, 128.41, 127.45, 127.04, 126.70, 126.03, 125.54, 124.15, 123.25, 121.63, 121.26, 121.20, 120.55, 120.46, 80.73, 31.84, 31.63, 30.65, 29.84, 29.62, 29.41, 29.30, 29.06, 28.41, 24.17, 22.79, 22.63, 14.26, 14.14. MS (MALDI-TOF): m/z [M^+] = 3296.5

General procedure for synthesis of BH2, BH4, and BH6. A 14 mL vial containing a stir bar was charged with ester (7, 8, or 9), methylene chloride (5 mL), and trifluoroacetic acid (1 mL) and the dark purple solution was allowed to stir (24ºC, 6 hours), solvent was removed in vacuo yielding pure BH2, BH4, or BH6 as black solids respectively in quantitative yields.

4-(bis(4-(5'-(2-(2,6-diisopropylphenyl)-1,3-dioxo-2,3-dihydro-1H-benzo[10,5]anthra[2,1,9-def]isoquinolin-8-yl)-3,4'-dihexyl-[2,2'-bithiophen]-5-yl)phenyl)amino)benzoic acid (BH2). Following the general procedure, Compound (7) (105mg, 53.3μmol) was stirred in methylene chloride and triflouroacetic acid to yield the title compound (102mg, quan.). M.P.: 201 ºC. ^{1}HNMR (400MHz, $CDCl_3$): δ = 8.70 (d, 4H, J = 8.02 Hz), 8.53 (m, 8H), 8.02 (d, 2H, J = 8.44 Hz), 7.97 (d, 2H, J = 8.88 Hz), 7.72 (d, 2H, J = 7.80 Hz), 7.67 (t, 2H, J = 7.96 Hz), 7.59 (d, 4H, J = 8.64 Hz), 7.49 (t, 2H, 7.74 Hz), 7.35 (d, 4H, J = 7.76 Hz), 7.23-7.16 (m, 7H), 7.13 (d, 2H, J = 8.88 Hz), 2.86 (t, 4H, J = 7.84 Hz), 2.78 (quin, 4H, J = 6.81 Hz), 2.46 (t, 4H, J = 7.65), 1.74 (quin, 4H J = 7.59), 1.62-1.52 (m, 4H), 1.49-1.40 (m, 4H), 1.39-1.31 (m, 10H), 1.19 (approx. s, 7H), 1.19 (approx. d, 39H, J = 6.84 Hz), 0.90 (t, 7H, J = 6.46 Hz), 0.78 (t, 6H, J = 6.96). ^{13}CNMR (400MHz, $CDCl_3$): δ = 164.23, 145.86, 145.65, 142.15, 141.19, 140.83, 137.83, 137.56, 136.29, 135.15, 134.07, 132.32, 131.93, 131.09, 130.68, 130.57, 130.19, 129.65, 129.55, 128.42, 127.49, 127.33, 127.06, 126.87, 126.26, 126.13, 124.30, 124.21, 123.36, 121.16, 121.09, 120.62, 120.53, 31.85, 31.64, 30.75, 30.62, 29.84, 29.43, 29.31, 29.18, 29.07, 24.16, 22.79, 22.63, 14.26, 14.15. MS (MALDI-TOF): m/z [M^+] = 1911.8

4-(bis(4-(5'''-(2-(2,6-diisopropylphenyl)-1,3-dioxo-2,3-dihydro-1H-benzo[10,5]anthra[2,1,9-def]isoquinolin-8-yl)-3,4',4'',4'''-tetrahexyl-[2,2':5',2'':5'',2'''-quaterthiophen]-5-yl)phenyl)amino)benzoic acid (BH4). Following the general procedure, Compound (8) (250mg, 94.9μmol) was stirred in methylene chloride and triflouroacetic acid to yield the title compound (245mg, quan.). M.P.: 199 ºC. ^{1}HNMR (400MHz, $CDCl_3$): δ = 8.70 (d, 4H J = 8.08 Hz), 8.58-8.50 (m, 8H), 8.02 (d, 2H, J = 8.96 Hz), 7.95 (d, 2H, J = 8.92 Hz), 7.72 (d, 2H, J = 7.76 Hz), 7.68 (t, 2H, J = 7.98 Hz), 7.60-7.54 (m, 4H), 7.48 (t, 2H, J = 7.80), 7.35 (d, 7.76 Hz), 7.22-7.09 (m, 10H), 7.03-6.98 (m, 4H), 2.89 (m, 15H), 2.46 (t, 3H, J = 7.52 Hz), 1.78-1.66 (m, 11H), 1.61-1.53 (m, 6H), 1.50-1.40 (m, 13H), 1.39-1.29 (m, 26H), 1.26 (s, 7H), 1.19 (approx. d, 40H J = 6.84 Hz), 0.94-0.87 (m, 20H), 8.02 (t, 6H, J = 8.96 Hz).). ^{13}CNMR (400MHz, $CDCl_3$): δ = 164.40, 145.83, 142.18, 141.05, 140.82, 140.12, 138.02, 137.75, 136.05, 135.29, 134.21, 134.13, 134.04, 132.48, 132.06, 130.95, 130.72, 130.58, 130.51, 130.28, 129.72, 129.50, 128.79, 128.40, 128.18, 127.51, 127.38, 127.06, 126.86, 126.20, 124.42, 124.27, 123.48, 120.92, 120.65, 120.56, 31.85, 31.63, 30.73, 30.67, 30.62, 29.79, 29.67, 29.42, 29.32, 29.19, 29.07, 24.14, 22.80, 22.64, 14.27, 14.15. MS (MALDI-TOF): m/z [M^+] = 2576.1

4-(bis(4-(5'''''-(2-(2,6-diisopropylphenyl)-1,3-dioxo-2,3-dihydro-1H-benzo[10,5]anthra[2,1,9-def]isoquinolin-8-yl)-3,4',4'',4''',4'''',4'''''-hexahexyl-[2,2':5',2'':5'',2''':5''',2'''':5'''',2'''''-sexithiophen]-5-yl)phenyl)amino)benzoic acid (BH6). Following the general procedure, Compound (9) (38mg, 11.5μmol) was stirred in methylene chloride and triflouroacetic acid to yield the title compound (37mg, quan.). M.P.: 168 ºC. ^{1}HNMR (400MHz, $CDCl_3$): δ = 8.72 (d, 4H, J = 7.92 Hz), 8.59-8.50 (m, 8H), 8.06 (d, 2H, J = 8.40 Hz), 7.99-7.91 (m, 2H), 7.74 (d, 2H, 7.68 Hz), 7.69 (t, 2H, J = 7.94 Hz), 7.62-7.54 (m, 3H), 7.50 (t, 3H, J = 7.78 Hz), 7.36 (d, 5H, J = 7.80 Hz), 7.23-6.91 (m, 17H), 2.90-2.72 (m, 20H), 2.47 (t, 4H, J = 7.40 Hz), 1.80-1.65 (m, 18H), 1.64-1.54 (m, 6H), 1.51-1.41 (m,18H), 1.40-1.29 (m, 46H), 1.27 (approx. s, 9H), 1.20 (approx. d, 45H, J = 6.80 Hz), 0.96-0.88 (m, 35H), 0.79 (t, 9H, J = 6.80 Hz). ^{13}CNMR (400MHz, $CDCl_3$): δ = 164.67, 145.79, 140.18, 138.32, 138.05, 134.03, 132.74, 132.20, 130.75, 130.72, 130.03, 129.84, 129.41, 129.35, 128.76, 128.36, 127.55,

127.05, 126.87, 126.29, 124.62, 124.36, 132.67, 120.68, 120.62, 31.85, 31.63, 30.67, 30.62, 29.85, 29.68, 29.42, 29.32, 29.19, 29.07, 24.11, 22.80, 22.63, 14.27, 14.14. MS (MALDI-TOF): m/z $[M^+]$ = 3240.4

DFT and TD-DFT Calculations

Gaussian 09 was used for all computational studies.[30] All BH dyes were optimized using density functional theory (DFT) with a 6-31G basis set. The optimum dihedral angle was found for a simpler oligiothiophene donor acceptor dye.[13] This dihedral angle was used as the dihedral angle between thiophenes in the BH dye series geometry optimizations. A vibrational frequency analysis was performed to confirm each BH dye as a minimum on the potential energy surface. The alkyl-side chains along the oligiothiophene was reduced from $-C_6H_{13}$ to $-C_3H_7$ to reduce computational expense.

Conclusions

We report three novel dyes, BH2, 4, and 6, for p-type DSCs, with BH4 yielding photocurrent up to 7.4 mA/cm^2, via a shorter synthetic scheme compared to a single acceptor design. It was found that in order to maximize the light absorption when building a dye containing a TPA donor it is beneficial to adopt a double acceptor design. In addition there was found to be a balance between the molar extinction coefficient and breadth of the dye. Also, the first reported light soaking effect for p-type DSSCs was observed. To date we have evidence that the source of the light soaking effect is based on the presence of lithium cations in the electrolyte. When lithium is replaced by larger cations (i.e. TBA and DMHII), no light soaking effect is observed. The mechanism for performance increase due to the light soaking effect reported is currently under detailed investigation.

Acknowledgement

The authors acknowledge the funding support from the U.S. Department of Energy (Award no. DE-FG02-07ER46427).

Notes and references

[*] *Department of Chemistry and Biochemistry, The Ohio State University,100 West 18th Avenue Columbus, Ohio 43210, USA. Fax: 614-292-1685; Tel: 614-247-7810; E-mail: wu@chemistry.ohio-state.edu*

† Electronic Supplementary Information (ESI) available: Detailed electrochemical and photochemical data. See DOI: 10.1039/b000000x/

‡ Indicates these authors contributed equally.

1. B. O'Regan and M. Grätzel, *Nature*, 1991, **353**, 737–740.

2. W. Shockley and H. J. Queisser, *J. Appl. Phys.*, 1961, **32**, 510.

3. A. De Vos, *J. Phys. D. Appl. Phys.*, 1980, **13**, 839–846.

4. S. Powar, T. Daeneke, M. T. Ma, D. Fu, N. W. Duffy, G. Götz, M. Weidelener, A. Mishra, P. Bäuerle, L. Spiccia, and U. Bach, *Angew. Chem. Int. Ed. Engl.*, 2013, **52**, 602–5.

5. M. Yu, G. Natu, Z. Ji, and Y. Wu, *J. Phys. Chem. Lett.*, 2012, **3**, 1074–1078.

6. a Nattestad, a J. Mozer, M. K. R. Fischer, Y.-B. Cheng, a Mishra, P. Bäuerle, and U. Bach, *Nat. Mater.*, 2010, **9**, 31–5.

7. P. Qin, H. Zhu, T. Edvinsson, G. Boschloo, A. Hagfeldt, and L. Sun, *J. Am. Chem. Soc.*, 2008, **130**, 8570–1.

8. Z. Ji, G. Natu, Z. Huang, and Y. Wu, *Energy Environ. Sci.*, 2011, **4**, 2818.

9. U. S. States, B. A. Gregg, S. Chen, and S. Ferrere, 2003, 3019–3029.

10. Q. Wang, Z. Zhang, S. M. Zakeeruddin, and M. Gra, 2008, 7084–7092.

11. E. Environ, A. Listorti, C. Creager, P. Sommeling, J. Kroon, E. Palomares, A. Fornelli, B. Breen, P. R. F. Barnes, J. R. Durrant, and B. O. Regan, 2011, 3494–3501.

12. L. Yang, B. Xu, D. Bi, H. Tian, G. Boschloo, L. Sun, A. Hagfeldt, and E. M. J. Johansson, *J. Am. Chem. Soc.*, 2013, **135**, 7378–85.

13. a Nattestad, a J. Mozer, M. K. R. Fischer, Y.-B. Cheng, a Mishra, P. Bäuerle, and U. Bach, *Nat. Mater.*, 2010, **9**, 31–5.

14. Z. Liu, W. Li, S. Topa, X. Xu, X. Zeng, Z. Zhao, M. Wang, W. Chen, F. Wang, Y.-B. Cheng, and H. He, *ACS Appl. Mater. Interfaces*, 2014, **6**, 10614–22.

15. S. Powar, Q. Wu, M. Weidelener, A. Nattestad, Z. Hu, A. Mishra, P. Bäuerle, L. Spiccia, Y.-B. Cheng, and U. Bach, *Energy Environ. Sci.*, 2012, **5**, 8896.

16. J. Cremer, E. Mena-Osteritz, N. G. Pschierer, K. Müllen, and P. Bäuerle, *Org. Biomol. Chem.*, 2005, **3**, 985–95.

17. J. Nishida, T. Masuko, Y. Cui, K. Hara, H. Shibuya, M. Ihara, T. Hosoyama, R. Goto, S. Mori, and Y. Yamashita, *J. Phys. Chem. C*, 2010, **114**, 17920–17925.

18. Y. Cui, Y. Wu, X. Lu, X. Zhang, G. Zhou, F. B. Miapeh, W. Zhu, and Z.-S. Wang, *Chem. Mater.*, 2011, **23**, 4394–4401.

19. P. Shen, Y. Liu, X. Huang, B. Zhao, N. Xiang, J. Fei, L. Liu, X. Wang, H. Huang, and S. Tan, *Dye. Pigment.*, 2009, **83**, 187–197.

20. J. E. Kroeze, N. Hirata, S. Koops, M. K. Nazeeruddin, L. Schmidt-Mende, M. Grätzel, and J. R. Durrant, *J. Am. Chem. Soc.*, 2006, **128**, 16376–83.

21. N. Koumura, Z.-S. Wang, S. Mori, M. Miyashita, E. Suzuki, and K. Hara, *J. Am. Chem. Soc.*, 2006, **128**, 14256–7.

22. A. Forneli, M. Planells, M. A. Sarmentero, E. Martinez-Ferrero, B. C. O'Regan, P. Ballester, and E. Palomares, *J. Mater. Chem.*, 2008, **18**, 1652.

23. M.-J. Kim, Y.-J. Yu, J.-H. Kim, Y.-S. Jung, K.-Y. Kay, S.-B. Ko, C.-R. Lee, I.-H. Jang, Y.-U. Kwon, and N.-G. Park, *Dye. Pigment.*, 2012, **95**, 134–141.

24. Z. Ji, G. Natu, Z. Huang, and Y. Wu, *Energy Environ. Sci.*, 2011, **4**, 2818.

25. S. Sumikura, S. Mori, S. Shimizu, H. Usami, and E. Suzuki, *J. Photochem. Photobiol. A Chem.*, 2008, **199**, 1–7.

26. L. Li, E. a Gibson, P. Qin, G. Boschloo, M. Gorlov, A. Hagfeldt, and L. Sun, *Adv. Mater.*, 2010, **22**, 1759–62.

27. M. He, Z. Ji, Z. Huang, and Y. Wu, *J. Phys. Chem. C*, 2014, 140227080825006.

28. L. Feiler, H. Langhals, and K. Polborn, *Liebigs Ann.*, 1995, **1995**, 1229–1244.

29. J. Baffreau, L. Ordronneau, S. Leroy-Lhez, and P. Hudhomme, *J. Org. Chem.*, 2008, **73**, 6142–7.

30. J. C. . and D. J. F. M. J. Frisch, G. W. Trucks, H. B. Schlegel, G. E. S.; M. dA. Robb, J. R. Cheeseman, G. Scalmani, V. Barone, B. M.; G. A. Petersson, H. Nakatsuji, M. Caricato, X. Li, H. P. H.; A. F. Izmaylov, J. Bloino, G. Zheng, J. L. Sonnenberg, M. H.; M. Ehara, K. Toyo, 2010.